America, northwestern Canada, Southeast Asia, and Africa. Other contributors to extreme AOD values include dust events in the Mediterranean and North Atlantic, and sea salt events near the Antarctic coast.

4) STRATOSPHERIC OZONE—M. Weber, W. Steinbrecht, S. M. Frith, O. Tweedy, M. Coldewey-Egbers, S. Davis, D. Degenstein, Y. E. Fioletov, L. Froidevaux, J. de Laat, C. S. Long, D. Loyola, C. Roth, and J. D. Wild

Total ozone columns in 2016 from GOME-2 were within a few Dobson units (DU) of the long-term (1998–2008) average for most of the globe (Plate 2.1s). At middle to high Northern Hemisphere (NH) latitudes total ozone was below the long-term average. The strong NH polar vortex observed during December 2015–February 2016, with record low temperatures and correspondingly large chlorine activation throughout, led to very low ozone values in the Arctic lower stratosphere during this period (not shown; Manney and Lawrence 2016). Very low stratospheric temperatures are needed to form polar stratospheric clouds (PSCs) that activate halogens (chlorine and bromine) for fast catalytic ozone depletion. Large ozone losses are regularly observed over Antarctica in the Southern Hemisphere (SH) spring (see Chapter 6h) but only sporadically over the Arctic. The observed Arctic ozone loss in early 2016 was comparable to or even stronger than the previous record loss during the Arctic winter 2010/11. Both winters showed Arctic ozone losses at levels typically only observed in the Antarctic ozone hole (Fig. 4 in WMO-GNR 2017; Manney et al. 2011).

In contrast, 2016 total ozone at middle to high SH latitudes was above average (Plate 2.1s) because of the below-average size of the Antarctic ozone hole in 2016 (see Chapter 6h). Both the size and intensity of ozone loss within the Antarctic vortex are variable and depend on the meteorology and atmospheric dynamics (transport) of any given winter.

At the equator there was a narrow band of slightly above-average total ozone (Plate 2.1s). Year-to-year variability of tropical total ozone is mainly governed by the phase of the quasi-biennial oscillation (QBO). The QBO is a periodic change of stratospheric winds in the lower to middle tropical stratosphere that affects the meridional (Brewer–Dobson) circulation and modulates high latitude ozone and the strength of the polar vortices (e.g., Strahan et al. 2015). In the 2015/16 boreal winter, radiosonde temperature observations revealed an unprecedented disruption in the downward propagation of the QBO westerly phase (Newman et al. 2016) that modified circulation and substantially impacted tropical and extratropical ozone (Tweedy et al. 2017). In Fig. 2.50, a "climatological" ozone QBO anomaly derived from deseasonalized SBUV Merged Ozone Data (MOD) V8.6 for 1982–2014 (14 QBO cycles) is compared to the ozone QBO evolution during late 2014–16. Each cycle is defined as starting when the vertical wind shear at 40 hPa shifts from negative (zonal wind decreasing with height) to positive. The long-term average evolution shows the typical increase in equatorial ozone associated with positive shear followed by a decrease associated with negative shear. The atypical cycle evolution in 2015/16 shows the anomalous equatorial ozone increase starting in June 2016.

The anomalous positive 40-hPa wind shear during April–November 2016 caused decreased tropical upwelling which led to a positive perturbation in tropical total ozone. This reduced upwelling was balanced by weaker extratropical downwelling, which decreased extratropical total ozone from April to September 2016. Total ozone shows markedly perturbed behavior in 2016 compared to the past, but the response of ozone and a variety of dynamical

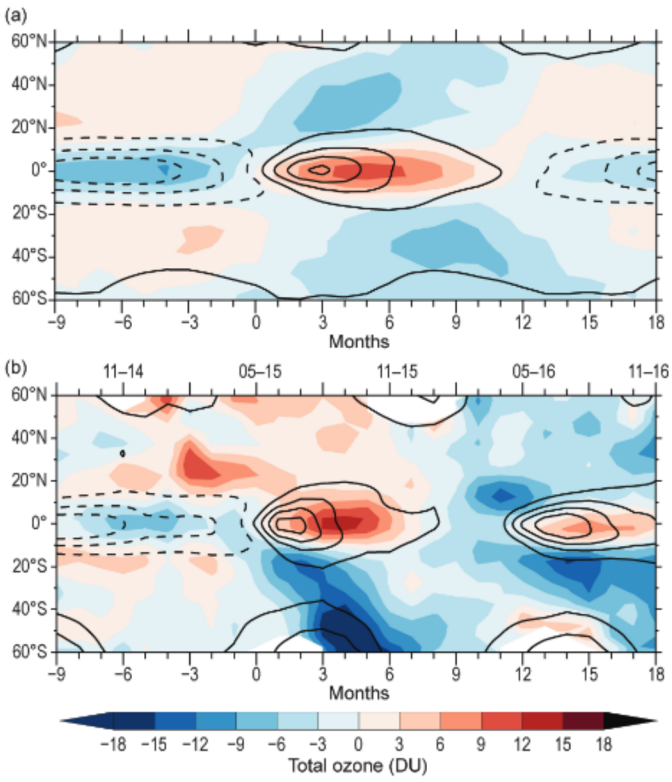

FIG. 2.50. Latitude–time evolution of the deseasonalized SBUV MOD V8.6 total ozone (color scale) for (a) the climatology of 14 QBO cycles (1982–2014) and (b) late 2014–16 (month–year indicated at the top). Solid and dashed black contours (interval is 2 m s^{-1} km^{-1}) show positive and negative vertical wind shear, respectively, for the composite and late 2014–16. Bottom axes show months before and after vertical wind shear changes from easterly to westerly at 40 hPa. Adapted from Tweedy et al. (2017).

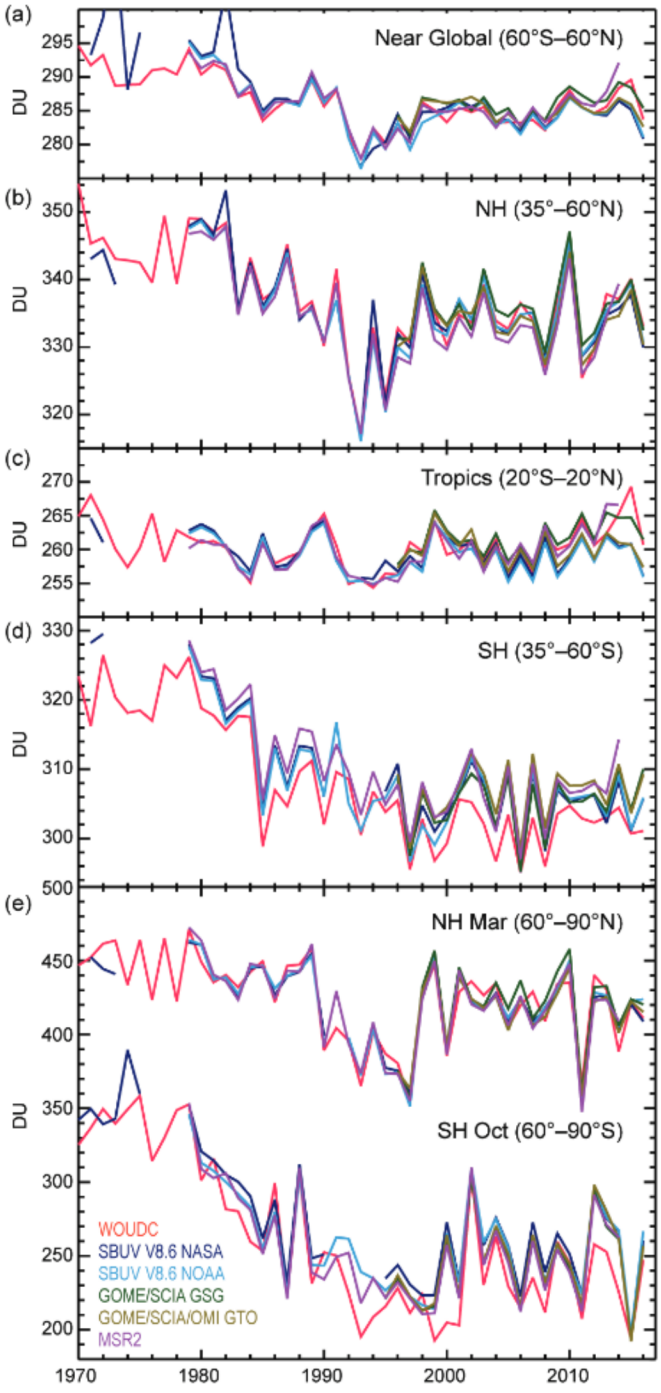

Fig. 2.51. Time series of annual mean total ozone in (a)–(d) four zonal bands and (e) polar (60°–90°) total ozone in Mar (NH) and Oct (SH). Data are from WOUDC ground-based measurements combining Brewer, Dobson, SAOZ, and filter spectrometer data (red; Fioletov et al. 2002, 2008); the BUV/SBUV/SBUV2 V8.6 merged products from NASA (MOD V8.6; dark blue; Chiou et al. 2014; Frith et al. 2014) and NOAA (light blue; Wild et al. 2016); the GOME/SCIAMACHY/GOME-2 products GSG from University of Bremen (dark green; Weber et al. 2011) and GTO from ESA/DLR (light green; Coldewey-Egbers et al. 2015); and the MSR V2 assimilated dataset extended with GOME-2 data (magenta; van der A et al. 2015). WOUDC values for 2016 are preliminary because not all ground station data were available at the time of writing this report.

and tracer fields is consistent with our understanding of the QBO-induced transport (Tweedy et al. 2017).

Time series of total column ozone annual means from different data sources are shown for 1970–2016 in various zonal bands (Fig. 2.51): near-global (60°N–60°S), middle latitudes in both hemispheres (35°–60°), and the inner tropics (20°N–20°S). Also shown are the polar time series in March (60°–90°N) and October (60°–90°S), the months when polar ozone losses are largest in the NH and SH, respectively (Fig. 2.51e). As a result of the early final warming in the Arctic (Manney and Lawrence 2016) and the breakup of the NH polar vortex, the 60°–90°N ozone levels in March 2016 quickly recovered to values close to the long-term mean despite the previously mentioned large chemical losses in early 2016.

Figure 2.51a shows that the continuous ozone decline due to the increase of ozone depleting substances (ODS) until the mid-1990s has ended. Since 2000 total ozone has leveled off in the extratropics of both hemispheres (Figs. 2.51b,d). Because the decline of ODS is slow (Section 2g2), ozone recovery is still difficult to separate from the considerable year-to-year variability. In the NH, tropical, and near-global averages, the annual mean ozone columns in 2016 were a few DU lower than those in the last couple of years, an expected result due to the declining phase of the 11-year solar cycle. Overall, the 2016 ozone columns are in agreement with expectations from

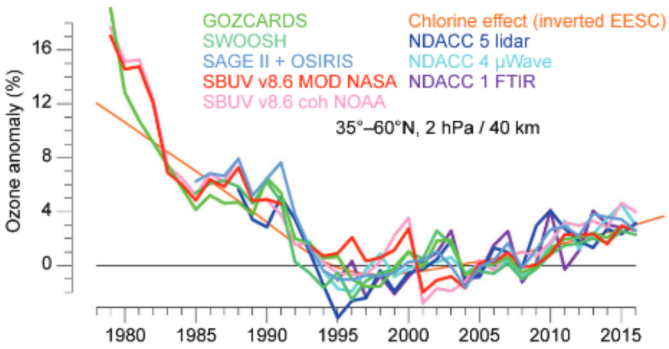

Fig. 2.52. Annual mean upper stratospheric ozone anomalies at 2 hPa (~40 km) in the zonal band 35°–60°N. Data are from the merged SAGE II/OSIRIS (Bourassa et al. 2014), GOZCARDS (Froidevaux et al. 2015), SWOOSH (Davis et al. 2016b), the BUV/SBUV/SBUV2 v8.6 merged products from NASA (Frith et al. 2014) and NOAA (Wild et al. 2016) as well as averages from five lidars, four microwave radiometers, and one FTIR measuring from the ground (Steinbrecht et al. 2009; Vigouroux et al. 2015). The anomaly basis for all time series is the 1998–2008 average of annual means. The thin orange curve represents EESC, inverted and scaled to reflect the expected ozone variations due to changes in stratospheric halogens. Data points for 2016 are still preliminary as of early 2017.

the last WMO Scientific Assessment of Stratospheric Ozone Depletion (WMO 2014).

The clearest signs of significant ozone recovery have occurred in the upper stratosphere at ~2 hPa/40 km (WMO 2014; Fig. 2.52). Both ground- and satellite-based measurements show recent increases of 2%–4% decade^{-1} in upper stratospheric ozone. At least in the upper stratosphere, adherence to the Montreal Protocol has successfully stopped the decline of stratospheric ozone and turned the previous downward trend into an upward trend since the late 1990s. Ensembles of chemistry–climate models indicate that the decline in stratospheric halogens and increases in greenhouse gases have contributed nearly equally to the positive ozone trend (WMO 2014).

5) Stratospheric water vapor—S. M. Davis, K. H. Rosenlof, D. F. Hurst, H. B. Selkirk, and H. Vömel

Stratospheric water vapor (SWV) levels varied dramatically during 2016. At the start of the year, water vapor mixing ratios in the tropical (15°N–15°S) lowermost stratosphere (at 82 hPa) were about 15% (0.5 ppm, parts per million mole fraction, equivalent to µmol mol^{-1}) above the previous decade's January average (Fig. 2.53). These positive anomalies followed the extremely high levels of SWV in November and December 2015 (Davis et al. 2016a; Fig. 2.54a) and the associated warm anomaly in cold point temperatures (CPTs) in the tropical tropopause layer (TTL) that began in mid-2015 and continued through the first two months of 2016 (Fig. 2.54b). The tropical SWV anomaly at 82 hPa in December 2015 (~0.9 ppm) is the highest observed in the now 13-year *Aura* Microwave Limb Sounder (MLS) record.

Between March and July 2016 the tropical SWV anomaly at 82 hPa dropped to ~0.2 ppm, then in August started to drop further, reaching –1.0 ppm in November 2016, the driest monthly anomaly observed in the *Aura* MLS record (Fig. 2.53b). Thus, from December 2015 to November 2016, the anomaly dropped by nearly 1.9 ppm, which is 40% of the long-term November mean tropical SWV mixing ratio at 82 hPa and 80% of the average seasonal cycle amplitude at 82 hPa in the tropics. In agreement with the MLS measurements, the steep water vapor decrease in the tropical lower stratosphere during 2016 was also observed by balloon-borne frost point hygrometer soundings at the tropical sites Hilo, Hawaii (20°N), and San José, Costa Rica (10°N) (Figs. 2.55b,c).

The annual cycle of tropical lower SWV is predominantly controlled by the annual cycle of CPTs in the TTL. These minimum temperatures are a major factor in determining the water vapor content of the lower stratosphere, because they impact the freeze–drying of moist tropospheric air during its slow ascent through the TTL. Seasonal to interannual variability in tropical SWV around 82 hPa is highly correlated with CPT variations. The dramatic decrease in tropical lower SWV during 2016 is consistent with the substantial ~1.5°C decrease in tropical CPTs over the same period (Fig. 2.55c).

Interannual variations in CPTs are partially related to interannual variability in the phases of ENSO and QBO in tropical stratospheric winds. At the beginning of 2016, the QBO was in a westerly (warm) phase at 70 hPa in the lowermost stratosphere, but an anomalous set of events brought descending easterlies to the tropical lower stratosphere during June–November 2016 (Newman et al. 2016; Osprey et al. 2016; Dunkerton 2016; Section 2e3). The colder TTL and drier tropical lower stratosphere at the end of 2016 is

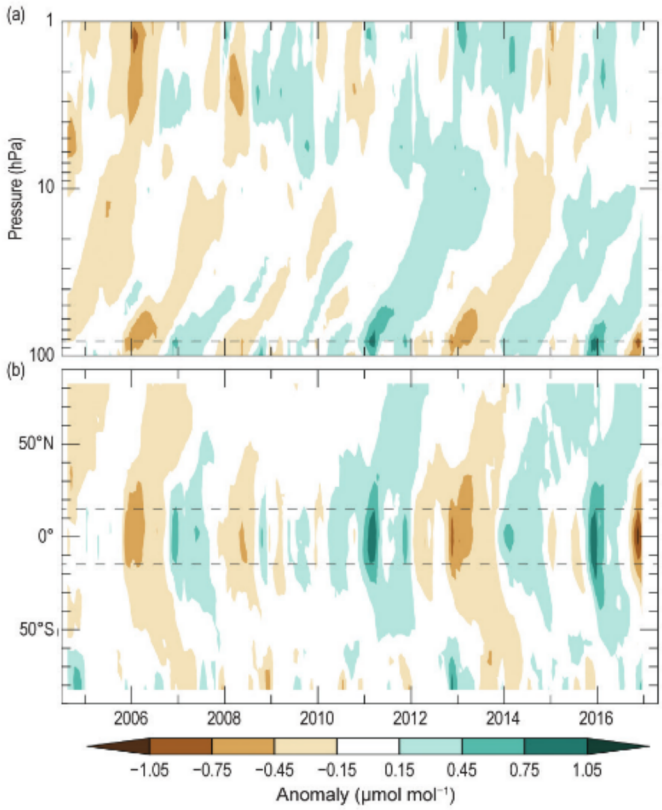

Fig. 2.53. (a) Time series of vertical profiles of tropical (15°N–15°S) stratospheric water vapor anomalies (µmol mol^{-1}) and (b) latitudinal distributions of SWV anomalies (µmol mol^{-1}) at 82 hPa. Both are based on *Aura* MLS data. Anomalies are differences from the mean 2004–2016 water vapor mixing ratios for each month. (b) Propagation of tropical lower SWV anomalies to higher latitudes in both hemispheres as well as the influences of dehydrated air masses from the Antarctic polar vortex as they are transported towards the SH midlatitudes at the end of each year. Dashed horizontal lines in the panels indicate (a) the 82-hPa pressure level and (b) the tropics 15°N–15°S.